# Large-scale automated synthesis of human functional neuroimaging data

Tal Yarkoni[1], Russell A Poldrack[2–4], Thomas E Nichols[5,6], David C Van Essen[7] & Tor D Wager[1]

**The rapid growth of the literature on neuroimaging in humans has led to major advances in our understanding of human brain function but has also made it increasingly difficult to aggregate and synthesize neuroimaging findings. Here we describe and validate an automated brain-mapping framework that uses text-mining, meta-analysis and machine-learning techniques to generate a large database of mappings between neural and cognitive states. We show that our approach can be used to automatically conduct large-scale, high-quality neuroimaging meta-analyses, address long-standing inferential problems in the neuroimaging literature and support accurate 'decoding' of broad cognitive states from brain activity in both entire studies and individual human subjects. Collectively, our results have validated a powerful and generative framework for synthesizing human neuroimaging data on an unprecedented scale.**

The development of noninvasive neuroimaging techniques such as functional magnetic resonance imaging (fMRI) has spurred rapid growth of literature on human brain imaging in recent years. In 2010 alone, more than 1,000 fMRI articles had been published[1]. This proliferation has led to substantial advances in our understanding of the human brain and cognitive function; however, it has also introduced important challenges. In place of too little data, researchers are now besieged with too much. Because individual neuroimaging studies are often underpowered and have relatively high false positive rates[2–4], multiple studies are required to achieve consensus regarding even broad relationships between brain and cognitive function. It is therefore necessary to develop new techniques for the large-scale aggregation and synthesis of human neuroimaging data[4–6].

Here we describe and validate a new framework for brain mapping, NeuroSynth, that takes an instrumental step toward automated large-scale synthesis of the neuroimaging literature. NeuroSynth combines text-mining, meta-analysis and machine-learning techniques to generate probabilistic mappings between cognitive and neural states that can be used for a broad range of neuroimaging applications. Whereas previous approaches have relied heavily on researchers' manual efforts (for example, refs. 7,8), which limits the scope and efficiency of resulting

analyses[1], our framework is fully automated and allows rapid and scalable synthesis of the neuroimaging literature. We show that this framework can be used to generate large-scale meta-analyses for hundreds of broad psychological concepts; support quantitative inferences about the consistency and specificity with which different cognitive processes elicit regional changes in brain activity; and decode and classify broad cognitive states in new data solely on the basis of observed brain activity.

## RESULTS
### Overview

Our methodological approach includes several steps (**Fig. 1a**). First, we used text-mining techniques to identify neuroimaging studies that used specific terms of interest (for example, 'pain', 'emotion', 'working memory' and so on) at a high frequency (>1 in 1,000 words) in the article text. Second, we automatically extracted activation coordinates from all tables reported in these studies. This approach produced a large database of term-to-coordinate mappings; here we report results based on 100,953 activation foci drawn from 3,489 neuroimaging studies published in 17 journals (Online Methods). Third, we conducted automated meta-analyses of hundreds of psychological concepts, producing an extensive set of whole-brain images that quantified relationships between brain activity and cognition (**Fig. 1b**). Finally, we used a machine-learning technique (naive Bayes classification) to estimate the likelihood that new activation maps were associated with specific psychological terms, which allowed relatively open-ended decoding of psychological constructs from patterns of brain activity (**Fig. 1c**).

### Automated coordinate extraction

Our approach differs from previous work in its heavy reliance on automatically extracted information, raising several potential concerns about data quality. For example, the software might incorrectly classify noncoordinate information in a table as an activation focus (a false positive); different articles report foci in different stereotactic spaces, resulting in potential discrepancies between anatomical locations represented by the same set of coordinates; and the software did not discriminate activations from deactivations.

[1]Department of Psychology and Neuroscience, University of Colorado at Boulder, Boulder, Colorado, USA. [2]Imaging Research Center, University of Texas at Austin, Austin, Texas, USA. [3]Department of Psychology, University of Texas at Austin, Austin, Texas, USA. [4]Department of Neurobiology, University of Texas at Austin, Austin, Texas, USA. [5]Department of Statistics, University of Warwick, Coventry, UK. [6]Warwick Manufacturing Group, University of Warwick, Coventry, UK. [7]Department of Anatomy and Neurobiology, Washington University School of Medicine, St. Louis, Missouri, USA. Correspondence should be addressed to T.Y. (tal.yarkoni@colorado.edu).
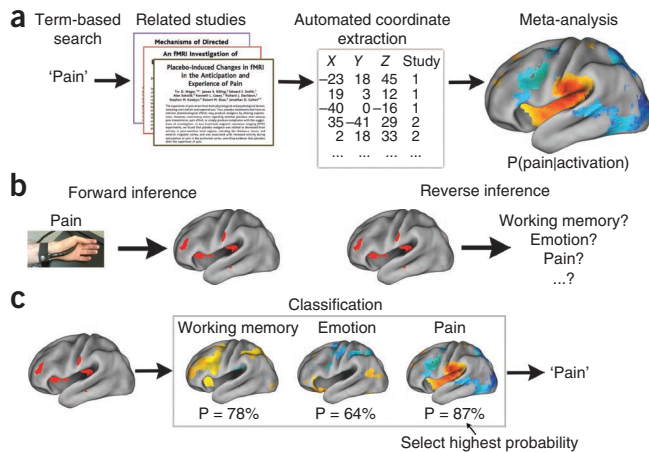
**Figure 1** | Schematic overview of NeuroSynth framework and applications. (**a**) Outline of the NeuroSynth approach. The full text of a large corpus of articles is retrieved and terms of scientific interest are stored in a database. Articles are retrieved from the database on the basis of a user-entered search string (for example, 'pain') and peak coordinates from the associated articles are extracted from tables. A meta-analysis of the peak coordinates is automatically performed, producing a whole-brain map of the posterior probability of the term given activation at each voxel (P(pain|activation)). (**b**) Outlines of forward and reverse inference in brain imaging. Given a known psychological manipulation, one can quantify the corresponding changes in brain activity and generate a forward inference, but given an observed pattern of activity, drawing a reverse inference about associated cognitive states is more difficult because multiple cognitive states could have similar neural signatures. (**c**) Given meta-analytic posterior probability maps for multiple terms (for example, working memory, emotion and pain), one can classify a new activation map by identifying the class with the highest probability, P, given the new data (in this example, pain).

To assess the effect of these issues on data quality, we conducted supporting analyses (**Supplementary Note**). First, we compared automatically extracted coordinates with a reference set of manually entered foci in the Surface Management System Database (SumsDB)[7,9], and found high rates of sensitivity (84%) and specificity (97%). Second, we quantified the proportion of activation increases versus decreases reported in the neuroimaging literature. We found that decreases constituted a small proportion of results and had minimal effect on our results. Third, we developed a preliminary algorithm (based on ref. 10) to automatically detect and correct for between-study differences in stereotactic space (**Supplementary Fig. 1**). Although automated extraction missed a minority of valid coordinates, and work remains to be done to increase the specificity of the extracted information, most coordinates were extracted accurately and several factors of a priori concern had relatively small influences on the results.

## Large-scale automated meta-analysis

We used the database of automatically extracted activation coordinates to conduct a comprehensive set of automated meta-analyses for several hundred terms of interest. For each term, we identified all studies that used the term at high frequency anywhere in the article text[11] and submitted all associated activation foci to a meta-analysis. This approach generated whole-brain maps that showed the strength of association between each term and every location in the brain, enabling us to make multiple kinds of quantitative inference (for example, if the term 'language' had been used in a study, how likely was the study to report activation in Broca's area? If activation had been observed in the amygdala, what was the probability that the study frequently used the term 'fear'?).

To validate this automated approach, which rests on the assumption that simple word counts are a reasonable proxy for the substantive content of articles, we conducted several supporting analyses (**Supplementary Note**). First, we found that NeuroSynth accurately recaptured conventional boundaries between distinct anatomical regions by comparing lexically defined regions of interest to anatomically defined regions of interest (**Supplementary Fig. 2**). Second, we used NeuroSynth to replicate previous findings of visual category-specific activation

**Figure 2** | Comparison of previous meta-analysis results with forward and reverse inference maps produced automatically using the NeuroSynth framework. (**a**) Meta-analytic maps produced manually in previous studies[14–16]. (**b**) Automatically generated forward inference maps showing the probability of activation given the presence of the term (P(act.|term)). (**c**) Automatically generated reverse inference maps showing the probability of the term given observed activation (P(term|act.)). Meta-analyses were carried out for working memory (top), emotion (middle) and physical pain (bottom) and mapped to the PALS-B12 atlas[30]. Regions in **b** were consistently associated with the term and regions in **c** were selectively associated with the term. To account for base differences in term frequencies, reverse inference maps assumed uniform priors (equal 50% probabilities of 'term' and 'no term'). Activation in orange or red regions implies a high probability that a term is present, and activation in blue regions implies a high probability that a term is not present. Values for all images are shown only for regions that survived a test of association between term and activation, with a whole-brain correction for multiple comparisons (false discovery rate was 0.05). DLPFC, dorsolateral prefrontal cortex; DACC, dorsal anterior cingulate cortex; AI, anterior insula.
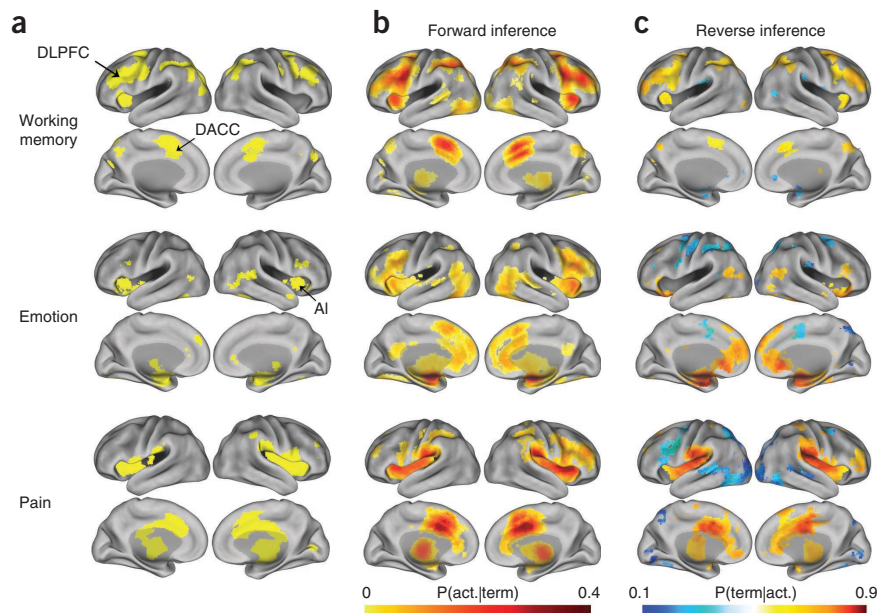
**Figure 3** | Comparison of forward and reverse inference in regions of interest. (**a**) Labeled regions of interest shown on lateral and medial brain surfaces. (**b**) Comparison of forward inference (probability of activation given term P(act.|term)) and reverse inference (probability of term given activation P(term|act.)) for the domains of working memory, emotion and pain as marked. * denotes results at a false discovery rate threshold of 0.05; (whole-brain false discovery rate, (*q*) = 0.05). DACC, dorsal anterior cingulate cortex (stereotactic coordinates in Montreal Neurological Institute space: +2, +8, +50); AI, anterior insula (+36, +16, +2); IFJ, inferior frontal junction (−50, +8, +36); PI, posterior insula (+42, −24, +24); APFC, anterior prefrontal cortex (−28, +56, +8); VMPFC, ventromedial prefrontal cortex (0, +32, −4). Dashed lines indicate even odds of a term being used (P(term|act.) = 0.5).

in regions such as the fusiform face area[12] and visual word form area[13] (**Supplementary Fig. 3**). Third, we found that more conservative meta-analyses in which the lexical search space had been restricted to article titles yielded similar, but less sensitive, meta-analysis results (**Supplementary Fig. 4**).

Finally, we compared our results with those produced by previous manual approaches. Comparison of automated meta-analyses of three broad psychological terms ('working memory', 'emotion' and 'pain') with previously published meta- or mega-analytic maps[14–16] revealed marked qualitative (**Fig. 2**) and quantitative convergence (**Supplementary Fig. 5**) between approaches. To directly test the convergence of automated and manual approaches when applied to similar data, we manually validated 265 automatically extracted pain studies and performed a standard multilevel kernel density analysis[15] to compare experimental pain stimulation with baseline (66 valid studies). There was a notable overlap between automated and manual results (correlation across voxels, 0.84; **Supplementary Fig. 6**). These results showed that, at least for broad domains, an automated meta-analysis approach generated results that were comparable in sensitivity and scope to those produced with more effort in previous studies.

## Quantitative reverse inference
The relatively comprehensive nature of the NeuroSynth database enabled us to address a long-standing inferential problem in the neuroimaging literature, namely how to quantitatively identify cognitive states from patterns of observed brain activity. This problem of 'reverse inference'[17] arises because most neuroimaging studies are designed to identify neural changes that result from known psychological manipulations and not to determine what cognitive state(s) a given pattern of activity implies[17] (**Fig. 1b**). For instance, fear consistently activates the human amygdala, but this does not imply that people in whom the amygdala is activated must be experiencing fear because other affective and nonaffective states have also been reported to activate the amygdala[4,18]. True reverse inference requires knowledge of which brain regions and networks are selectively, and not just consistently, associated with particular cognitive states[15,17].

Because the NeuroSynth database contains a broad set of term-to-activation mappings, our framework is well suited for drawing quantitative inferences about mind-brain relationships in both the forward and reverse directions. We could quantify both the probability that there would be activation in specific brain regions given the presence of a particular term (P(activation|term) or 'forward inference'), and the probability that a term would occur in an
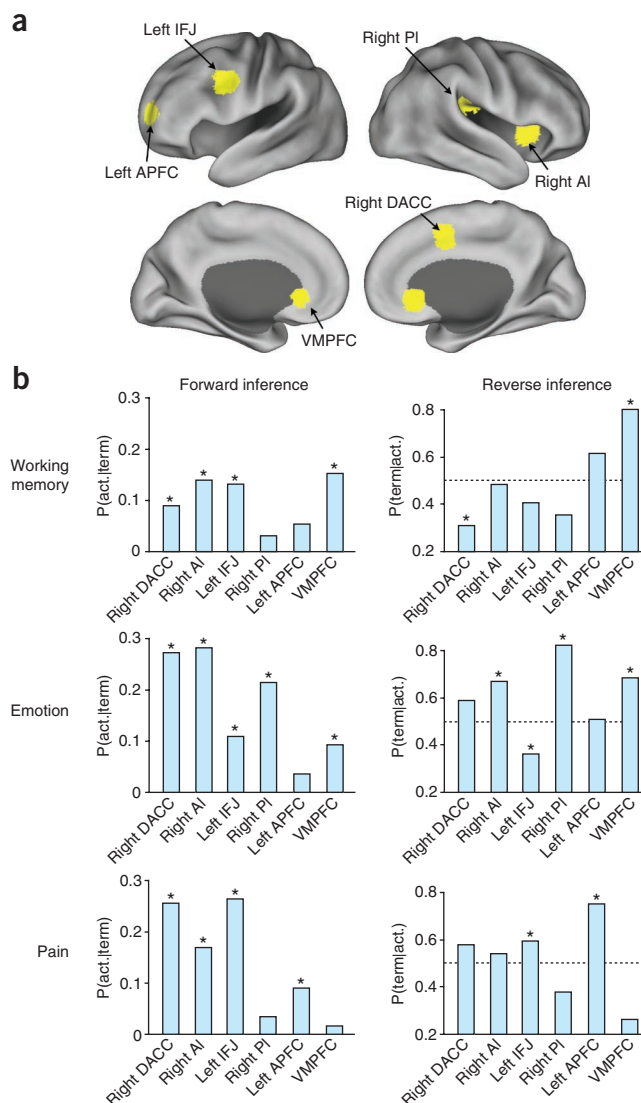
article given the presence of activation in a particular brain region (P(term|activation) or reverse inference). Comparison of these two analyses allowed us to assess the validity of many common inferences about the relationship between neural and cognitive states.

For illustration, we focused on the sample domains of working memory, emotion and pain, which are of substantial basic and clinical interest and have been extensively studied using fMRI (for additional examples, see **Supplementary Fig. 7**). These domains are excellent candidates for quantitative reverse inference, as they are thought to have confusable neural correlates, with common activation of regions such as the dorsal anterior cingulate cortex (DACC)[19] and anterior insula.

Our results showed differences between the forward and reverse inference maps in all three domains (**Fig. 2**). For working memory, the forward inference map revealed the most consistent associations in the dorsolateral prefrontal cortex, anterior insula and dorsal medial frontal cortex, replicating previous findings[15,20]. However, the reverse inference map instead implicated the anterior prefrontal cortex and posterior parietal cortex as the regions that were most selectively activated by working memory tasks.

We observed a similar pattern for pain and emotion. In both domains, frontal regions that have been broadly implicated in

**Figure 4** | Three-way classification of working memory, emotion and pain. (**a**) Naive Bayes classifier performance when cross-validated on studies in the database (left) or applied to individual subjects from studies not in the database (right). (**b**) Whole-brain maximum posterior probability map; each voxel is colored by the term with the highest associated probability. (**c**) Whole-brain maps showing the proportion of individual subjects in the three pain studies ($n = 79$ subjects total) who showed activation at each voxel ($P < 0.05$, uncorrected), averaged separately for subjects who were classified correctly ($n = 51$ subjects; top) or incorrectly ($n = 28$ subjects; bottom). Regions are color-coded according to the proportion of subjects in the sample who showed activation at each voxel.
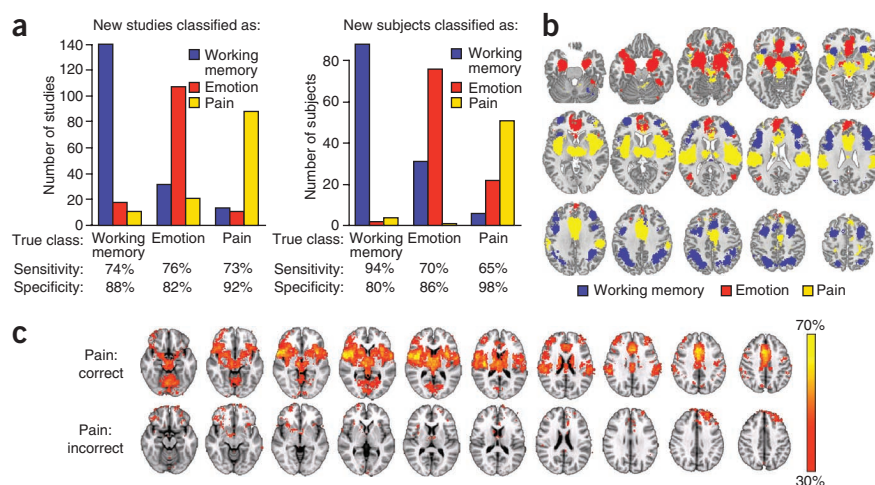
goal-directed cognition[21–23] showed consistent activation in the forward analysis but were relatively nonselective in the reverse analysis (**Fig. 2**). For emotion, the reverse inference map revealed much more selective activation in the amygdala and ventromedial prefrontal cortex (**Fig. 3**). For pain, the regions of maximal pain-related activation in the insula and DACC shifted from anterior foci in the forward analysis to posterior ones in the reverse analysis (**Fig. 3**). This is consistent with studies of nonhuman primates that have implicated the dorsal posterior insula as a primary integration center for nociceptive afferents[24] and with studies of humans in which anterior aspects of the so-called 'pain matrix' responded nonselectively to multiple modalities[25].

Several frontal regions that showed consistent activation for emotion and pain in the forward analysis were associated with a decreased likelihood that a study involved emotion or pain in the reverse inference analysis (**Fig. 3**). This seeming paradox reflected the fact that even though lateral and medial frontal regions had been consistently activated in studies of emotion and pain, they had been activated even more frequently in studies that did not involve emotion or pain (**Supplementary Fig. 8**). Thus, the fact that these regions showed involvement in pain and emotion probably reflected their much more general role in cognition (for example, sustained attention or goal-directed processing[22,23]) rather than processes specific to pain or emotion.

These results showed that without the ability to distinguish consistency from selectivity, neuroimaging data can produce misleading inferences. For instance, neglecting the high base rate of DACC activity might lead researchers in the areas of cognitive control, pain and emotion to conclude that the DACC has a key role in each domain. Instead, because the DACC is activated consistently in all of these states, its activation may not be diagnostic of any one of them and conversely, might even predict their absence. The NeuroSynth framework can potentially address this problem by enabling researchers to conduct quantitative reverse inference on a large scale.

### Open-ended classification of cognitive states

An emerging frontier in human neuroimaging is brain 'decoding': inferring a person's cognitive state from their observed brain activity. The problem of decoding is essentially a generalization of the univariate reverse inference problem addressed above: instead of predicting the likelihood of a particular cognitive state given activation at a single voxel, one can generate a corresponding prediction based on an entire pattern of brain activity. The NeuroSynth framework is well positioned for such an approach: whereas previous decoding approaches have focused on discriminating between narrow sets of cognitive states and have required extensive training on raw fMRI datasets (for example, refs. 26–28), the breadth of cognitive concepts represented in the NeuroSynth database affords relatively open-ended decoding, with little or no training on new datasets.

To assess the ability of our approach to decode and classify cognitive states, we trained a naive Bayes classifier[29] that could discriminate between flexible sets of cognitive states given new images as input (**Fig. 1c**). First, we tested the classifier's ability to classify studies in the NeuroSynth database that had been associated with different terms. In a tenfold cross-validated analysis, the classifier discriminated between studies of working memory, emotion and pain with high sensitivity and specificity (**Fig. 4a**), showing that each of these domains had a relatively distinct neural signature (**Fig. 4b**).

To assess the classifier's ability to decode cognitive states in individual human subjects, we applied the classifier to 281 single-subject activation maps derived from contrasts between: n-back working memory performance and rest (94 maps); negative and neutral emotional photographs (108 maps); and intense and mild thermal pain (79 maps). The classifier performed substantially above chance, identifying the originating study type with sensitivities of 94%, 70% and 65%, respectively (chance = 33%), and specificities of 80%, 86% and 98% (**Fig. 4a**). Moreover, there were systematic differences in activation patterns for correctly and incorrectly classified subjects. For example, incorrectly classified subjects in physical pain tasks (**Fig. 4c**) systematically activated the lateral orbitofrontal cortex and dorsomedial prefrontal cortex but not secondary somatosensory cortex or the posterior insula, suggesting that the discomfort owing to noxious heat in these subjects may have been qualitatively different (for example, emotionally generated versus physically generated pain). Thus, these findings demonstrate the viability of decoding cognitive states in new subjects without training and suggest new hypotheses for exploration.

Next, to generalize beyond working memory, emotion and pain, we selected 25 broad psychological terms that occurred at high frequency in the database (**Fig. 5**). We estimated classification accuracy in tenfold cross-validated two-alternative and multiclass analyses. The classifier performed substantially above

**Figure 5** | Accuracy of the naive Bayes classifier when discriminating between all possible pairwise combinations of 25 key terms. Each cell represents a cross-validated binary classification between the intersecting row and column terms. Off-diagonal values reflect accuracy averaged across the two terms. Diagonal values reflect the mean classification accuracy for each term. Terms were ordered using the first two factors of a principal components analysis. All accuracy rates above 58% and 64% are statistically significant at $P < 0.05$ and $P < 0.001$, respectively.
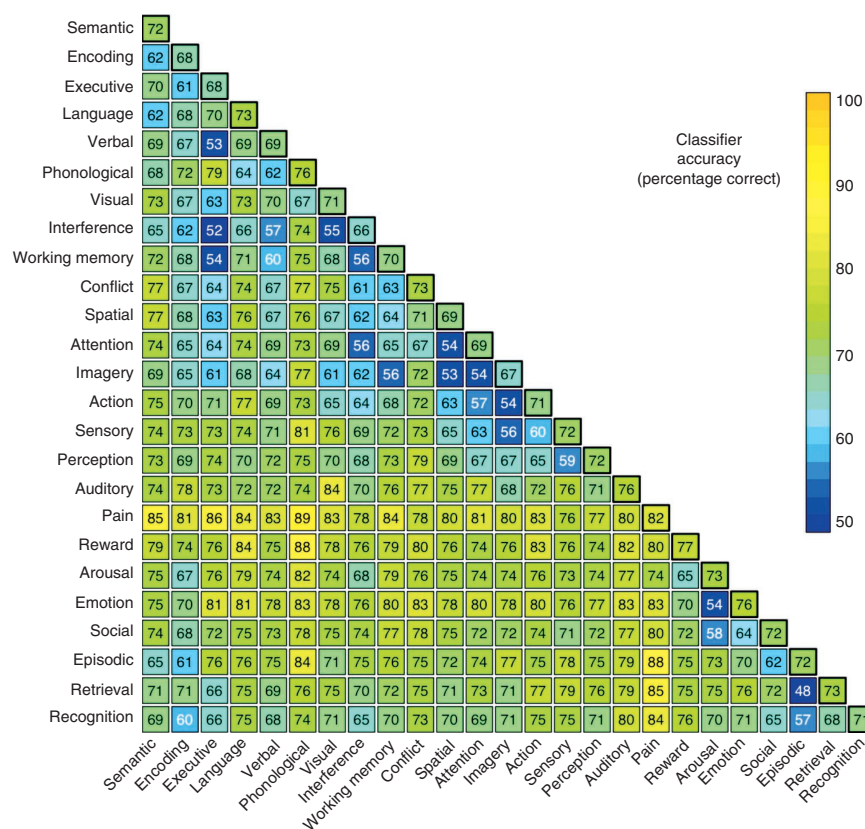
chance in both two-alternative classification (mean pairwise accuracy of 72%; **Fig. 4**) and relatively open-ended multiclass classification on up to ten simultaneous terms (**Supplementary Fig. 9**). The results provided insights into the similarity structure of neural representation for different processes. For instance, pain was highly discriminable from other psychological concepts (all pairwise accuracies > 74%), which suggests that pain perception might be a distinctive state that is grouped neither with other sensory modalities nor with other affective concepts such as arousal and emotion. Conversely, conceptually related terms such as 'executive' and 'working memory' could not be distinguished at a rate different from chance, reflecting their closely overlapping usage in the literature.

## DISCUSSION

Using the NeuroSynth framework, first we conducted large-scale automated neuroimaging meta-analyses of broad psychological concepts that are lexically well represented in literature. A key benefit of NeuroSynth is the ability to quantitatively distinguish forward inference from reverse inference, which should allow researchers to assess the specificity of mappings between neural and cognitive function, a long-standing goal of cognitive neuroscience research. Although considerable work remains to be done to improve the specificity and accuracy of the tools developed here, we expect quantitative reverse inference to be increasingly important in future meta-analytic studies.

Second, we decoded broad psychological states in a relatively open-ended way in individual subjects; this was, to our knowledge, the first application of a domain-general classifier that can distinguish a broad range of cognitive states based solely on prior literature. The ability to decode brain activity without previous training data or knowledge of the 'ground truth' for an individual is particularly promising. Our results raise the prospect that legitimate 'mind reading' of more nuanced cognitive and affective states might eventually become feasible with additional technical advances. However, the present NeuroSynth implementation provides no basis for such inferences, as it distinguishes only between relatively broad psychological categories.

Third, we designed our platform to support immediate use in a broad range of neuroimaging applications. To name just a few potential applications, researchers could use these tools and

results to define region-of-interest masks or Bayesian priors in hypothesis-driven analyses; to conduct quantitative comparisons between meta-analysis maps of different terms of interest; to use the automatically extracted coordinate database as a starting point for more refined manual meta-analyses; to draw more rigorous reverse inferences when interpreting results by referring to empirically established mappings between specific regions and cognitive functions; and to extract the terms that are most frequently associated with an active region or distributed pattern of activity, thereby contextualizing new research findings on the basis of published data.

Of course, the NeuroSynth framework is not a panacea for the many challenges that face cognitive neuroscientists, and several limitations remain to be addressed. We focus on two in particular here. First, the present reliance on a purely lexical coding approach, albeit effective, is suboptimal in that it relies on traditional psychological terms that do not carve the underlying neural substrates at their natural joints, do not capitalize on redundancy across terms (for example, 'pain', 'nociception' and 'noxious' overlap closely but are modeled separately) and do not allow closely related constructs to be easily distinguished (for example, physical versus emotional pain). Future efforts could overcome these limitations by using controlled vocabularies or ontologies for query expansion, developing extensions for conducting multiterm analyses and extracting topic-based representations of article text (**Supplementary Note**).

Second, although our automated tools accurately extract coordinates from articles, they cannot extract information about fine-grained cognitive states (for example, different negative emotions). Thus, the NeuroSynth framework is currently useful primarily for large-scale analyses involving broad domains and

should be viewed as a complement to, and not as a substitute for, manual meta-analysis approaches. We are currently working to develop improved algorithms for automatic coding of experimental contrasts, which should substantially improve the specificity of the resulting analyses. In parallel, we envision a 'crowd-sourced' collaborative model in which multiple groups participate in the validation of automatically extracted data, thereby combining the best elements of both automated and manual approaches. Such efforts should further increase the specificity and predictive accuracy of the decoding model, and we hope that they will lead to the development of many other applications that we have not anticipated here.

To encourage application and development of a synthesis-oriented approach, we have publicly released most of the tools and data used in the present study through a web interface (http://neurosynth.org/). We hope that cognitive neuroscientists will use, and contribute to, this new resource, with the goal of developing new techniques for interpreting and synthesizing the wealth of data generated by modern neuroimaging techniques.

## METHODS
Methods and any associated references are available in the online version of the paper at http://www.nature.com/naturemethods/.

*Note: Supplementary information is available on the Nature Methods website.*

### AUTHOR CONTRIBUTIONS
T.Y. conceived the project and carried out most of the software implementation, data analysis and writing. R.A.P. provided data and performed analyses. T.E.N. provided statistical advice, reviewed all statistical procedures and contributed to the implementation of the naive Bayes classifier. D.C.V.E. provided data, contributed to automated data extraction and coordinated data validation. T.D.W. conceived the classification analyses, wrote part of the software, provided data and suggested and performed analyses. All authors contributed to writing and editing the manuscript.

### COMPETING FINANCIAL INTERESTS
The authors declare no competing financial interests.

**Published online at http://www.nature.com/naturemethods/.**
**Reprints and permissions information is available online at http://www.nature.com/reprints/index.html.**

1.  Derrfuss, J. & Mar, R.A. Lost in localization: the need for a universal coordinate database. *Neuroimage* **48**, 1–7 (2009).
2.  Yarkoni, T. Big correlations in little studies: inflated fMRI correlations reflect low statistical power—commentary on Vul *et al.* (2009). *Perspect. Psychol. Sci.* **4**, 294–298 (2009).
3.  Wager, T.D., Lindquist, M. & Kaplan, L. Meta-analysis of functional neuroimaging data: current and future directions. *Soc. Cogn. Affect. Neurosci.* **2**, 150–158 (2007).
4.  Yarkoni, T., Poldrack, R.A., Van Essen, D.C. & Wager, T.D. Cognitive neuroscience 2.0: building a cumulative science of human brain function. *Trends Cogn. Sci.* **14**, 489–496 (2010).
5.  Van Horn, J.D., Grafton, S.T., Rockmore, D. & Gazzaniga, M.S. Sharing neuroimaging studies of human cognition. *Nat. Neurosci.* **7**, 473–481 (2004).
6.  Fox, P.T., Parsons, L.M. & Lancaster, J.L. Beyond the single study: function/location metanalysis in cognitive neuroimaging. *Curr. Opin. Neurobiol.* **8**, 178–187 (1998).
7.  Van Essen, D.C. Lost in localization—but found with foci?! *Neuroimage* **48**, 14–17 (2009).
8.  Laird, A.R. *et al.* ALE meta-analysis workflows via the BrainMap database: progress towards a probabilistic functional brain atlas. *Front Neuroinformatics* **3**, 23 (2009).
9.  Dickson, J., Drury, H.A. & Van Essen, D.C. "The surface management system" (SuMS) database: a surface-based database to aid cortical surface reconstruction, visualization and analysis. *Phil. Trans. R. Soc. Lond. B* **356**, 1277–1292 (2001).
10. Lancaster, J.L. *et al.* Bias between MNI and Talairach coordinates analyzed using the ICBM-152 brain template. *Hum. Brain Mapp.* **28**, 1194–1205 (2007).
11. Nielsen, F.A., Hansen, L.K. & Balslev, D. Mining for associations between text and brain activation in a functional neuroimaging database. *Neuroinformatics* **2**, 369–380 (2004).
12. Kanwisher, N., McDermott, J. & Chun, M.M. The fusiform face area: a module in human extrastriate cortex specialized for face perception. *J. Neurosci.* **17**, 4302–4311 (1997).
13. McCandliss, B.D., Cohen, L. & Dehaene, S. The visual word form area: expertise for reading in the fusiform gyrus. *Trends Cogn. Sci.* **7**, 293–299 (2003).
14. Atlas, L.Y., Bolger, N., Lindquist, M.A. & Wager, T.D. Brain mediators of predictive cue effects on perceived pain. *J. Neurosci.* **30**, 12964–12977 (2010).
15. Wager, T.D., Lindquist, M.A., Nichols, T.E., Kober, H. & Van Snellenberg, J.X. Evaluating the consistency and specificity of neuroimaging data using meta-analysis. *Neuroimage* **45**, 210–221 (2009).
16. Kober, H. *et al.* Functional grouping and cortical-subcortical interactions in emotion: a meta-analysis of neuroimaging studies. *Neuroimage* **42**, 998–1031 (2008).
17. Poldrack, R.A. Can cognitive processes be inferred from neuroimaging data? *Trends Cogn. Sci.* **10**, 59–63 (2006).
18. Zald, D.H. The human amygdala and the emotional evaluation of sensory stimuli. *Brain Res. Brain Res. Rev.* **41**, 88–123 (2003).
19. Shackman, A.J. *et al.* The integration of negative affect, pain and cognitive control in the cingulate cortex. *Nat. Rev. Neurosci.* **12**, 154–167 (2011).
20. Owen, A.M., McMillan, K.M., Laird, A.R. & Bullmore, E. N-back working memory paradigm: a meta-analysis of normative functional neuroimaging studies. *Hum. Brain Mapp.* **25**, 46–59 (2005).
21. Dosenbach, N.U. *et al.* A core system for the implementation of task sets. *Neuron* **50**, 799–812 (2006).
22. Duncan, J. The multiple-demand (MD) system of the primate brain: mental programs for intelligent behaviour. *Trends Cogn. Sci.* **14**, 172–179 (2010).
23. Yarkoni, T., Barch, D.M., Gray, J.R., Conturo, T.E. & Braver, T.S. BOLD correlates of trial-by-trial reaction time variability in gray and white matter: a multi-study fMRI analysis. *PLoS ONE* **4**, e4257 (2009).
24. Craig, A.D. How do you feel? Interoception: the sense of the physiological condition of the body. *Nat. Rev. Neurosci.* **3**, 655–666 (2002).
25. Legrain, V., Iannetti, G.D., Plaghki, L. & Mouraux, A. The pain matrix reloaded: a salience detection system for the body. *Prog. Neurobiol.* **93**, 111–124 (2011).
26. Norman, K.A., Polyn, S.M., Detre, G.J. & Haxby, J.V. Beyond mind-reading: multi-voxel pattern analysis of fMRI data. *Trends Cogn. Sci.* **10**, 424–430 (2006).
27. Mitchell, T.M. *et al.* Predicting human brain activity associated with the meanings of nouns. *Science* **320**, 1191–1195 (2008).
28. Poldrack, R.A., Halchenko, Y.O. & Hanson, S.J. Decoding the large-scale structure of brain function by classifying mental states across individuals. *Psychol. Sci.* **20**, 1364–1372 (2009).
29. Lewis, D. Naive (Bayes) at forty: The independence assumption in information retrieval. *Mach. Learn.* **ECML-98**, 4–15 (1998).
30. Lang, P.J., Bradley, M.M. & Cuthbert, B.N. *International Affective Picture System (IAPS): Instruction Manual and Affective Ratings* (Center for Research in Psychophysiology, University of Florida, Gainesville, Florida, USA, 1999).

## ONLINE METHODS

**Automated coordinate extraction.** To automatically extract stereotactic coordinate information from published neuroimaging articles, we developed a software library written in the Ruby programming language. We released the NeuroSynth automated coordinate extraction (ACE) tools under an open-source license and encourage other researchers to contribute to the codebase (http://github.com/neurosynth/). Because the code is freely available for inspection and use, we provide only a functional, nontechnical overview of the tools here.

In brief, ACE consists of a parsing engine that extracts coordinate information from published articles by making educated guesses about the contents of the columns reported in tables in neuroimaging articles (at present, ACE does not attempt to extract coordinates that are reported in the main text of an article or in supplementary materials). For each full-text HTML article provided as input, ACE scans all tables for rows that contain coordinate-like data. Rows or tables that do not contain values that correspond to a flexible template used to detect coordinates are ignored. Moreover, all extracted coordinates are subjected to basic validation to ensure that they reflect plausible locations in stereotactic space (for example, all coordinates with absolute values > 100 in any plane are discarded).

Although neuroimaging coordinates are reported in a variety of stereotactic spaces in the neuroimaging literature[31,32], for technical reasons, the results we reported in the main text ignore such differences and collapse across different spaces. Moreover, the parser did not distinguish activations from deactivations, and aggregates across all reported contrasts in each article, that is, it makes no attempt to code different tables within an article, or different contrasts within a table, separately. As extensive validation analyses showed (**Supplementary Note**), these factors appear to exert only a modest influence on results, and in some cases can be automatically accounted for; however, for present purposes we simply note that the net effect of these limitations should be to reduce fidelity rather than to introduce systematic bias.

As well as extracting coordinates, ACE parses the body of each article and generates a list of all words that appear at least once anywhere in the text, along with a corresponding frequency count for each word. All data are then stored in a relational (MySQL) database that maintains associations between words, articles and activation foci, allowing flexible and powerful structured retrieval of information.

**Database.** The foci used to generate the results of the present study were extracted from 17 source journals: *Biological Psychiatry, Brain, Brain and Cognition, Brain and Language, Brain Research, Cerebral Cortex, Cognitive Brain Research, Cortex, European Journal of Neuroscience, Human Brain Mapping, Journal of Neurophysiology, Journal of Neuroscience, NeuroImage, NeuroLetters, Neuron, Neuropsychologia* and *Pain*. We deliberately focused on journals that contained a high incidence of functional neuroimaging studies; thus, some important general neuroscience or science journals (for example, *Science, Nature* and *Nature Neuroscience*) were not included. The range of years represented varied by journal, with the earliest studies dating to 2000 and the latest to early 2010. The database contains 3,489 articles and 100,953 foci, and is, to our knowledge, the largest extant database of neuroimaging foci, though it still captures only a minority of the published literature[1].

The database has considerable potential for additional growth. Because neuroimaging studies appear in dozens of journals (besides those analyzed here), which typically require the use of publisher-specific or journal-specific filters to correctly obtain coordinates from tables, the database will continue to grow as new filters are added. An additional limitation is that many journals have not yet made full-text HTML versions of older articles available online; as such efforts proceed, the database will grow correspondingly. Finally, because authors report coordinate information in a variety of formats, false negatives can occur (that is, ACE might not extract real coordinate information). However, these limitations do not bias the present analyses in any particular way, and suggest that if anything, one can expect the sensitivity and specificity of the reported results to improve as the database grows and additional quality assurance procedures are implemented.

**Statistical inference and effect size maps.** In keeping with previous meta-analyses that used multilevel kernel density analysis (MKDA[15]), we represented reported activations from each study by constructed a binary image mask, with a value of 1 (reported) assigned to each voxel in the brain if it was within 10 mm of a focus reported in that article and 0 (not reported) if it was not within 10 mm of a reported focus[15]. These maps used 2 mm × 2 mm × 2 mm voxels, with $n_V = 231,202$ voxels in the brain mask. We denote the activation map for study $i$ as $A_i = (A_{ij})$, a length-$n_V$ binary vector.

A frequency cut-off of 0.001 was used to eliminate studies that only used a term incidentally (that is, to be considered about pain, a study had to use the term 'pain' at a rate of at least one in every 1,000 words). Subsequent testing revealed that the results were largely insensitive to the exact cut-off used (including no cut-off at all), except that very high cut-offs (for example, 0.01 or higher) tended to leave too few studies for reliable estimation of most terms. (As the database grows, even very conservative thresholds that leave no ambiguity at all about the topic of a study should become viable.) The total number of terms collected was $n_T = 10,000$ (although the majority of these were nonpsychological in meaning—for example, 'activation' and 'normal'). We write the term indicator for study $i$ as $T_i = (T_{ik})$, a length-$n_T$ binary vector marking each term 'present' (frequency above the cut-off) or 'absent' (frequency below the cut off).

For each term of interest in the database (for example, 'pain', 'amygdala') we generated whole-brain meta-analysis maps that showed the strength of statistical association between the term and reported activation at each voxel. For each voxel $j$ and term $k$, every study can be cross-classified by activation (present or absent) and term (present or absent), producing a 2 × 2 contingency table of counts.

Statistical inference maps were generated using a $\chi^2$ test of independence, with a significant result implying the presence of a dependency between term and activation (that is, a change in activation status would make the occurrence of the term more or less likely). This approach departs from the MKDA approach used in previous meta-analyses[3,15,16] in its reliance on a parametric statistical test in place of permutation-based family wise error rate (FWE) correction; however,

permutation-based testing was not computationally feasible given the scale of the present meta-analyses (multiple maps for each of several thousand terms).

To stabilize results and to ensure that all cells had sufficient observations for the parametric $\chi^2$ test, we excluded all voxels that were active in fewer than 3% of studies (**Supplementary Fig. 10**). The resulting *P*-value map was false discovery rate (FDR)-corrected for multiple comparisons using a whole-brain FDR threshold of 0.05, identifying voxels where there was significant evidence that term frequency varied with activation frequency. Intuitively, one can think of regions that survive correction as those that show differential activation for studies that include a term versus studies that do not include that term.

We also computed maps of the posterior probability that term *k* was used in a study given activation at voxel *j*

$$P(T_k = 1 \mid A_j = 1) = P(A_j = 1 \mid T_k = 1)P(T_k = 1) / P(A_j)$$

(generically referred to as P(Term|Activation) in the text). We use the 'smoothed' estimates for the likelihood of activation given the term

$$p(A_j = 1 \mid T_k = 1) = \left( \sum_i A_{ij}T_{ik} + m\mathrm{p} \right) \bigg/ \left( \sum_i T_{ik} + m \right)$$

where p($\cdot$) reflects an estimated versus true probability, *m* is a virtual equivalent sample size and p is a prior probability. The parameters *m* and p are set equal to 2 and 0.5, respectively; this smoothing was equivalent to adding two virtual studies that have term *k* present, one having an activation one, one without. This regularization prevents rare activations or terms from degrading accuracy[33]. For P($T_k = 1$) we impose a uniform prior for all terms, P($T_k = 1$) = P($T_k = 0$) = 0.5. We use this uniform prior because terms differed widely in frequency of usage, leading to very different posterior probabilities for different terms. This is equivalent to making an assumption that the usage and nonusage of the term would be equally likely in the absence of any knowledge about brain activation. Note that this is a conservative approach; using uniform priors will tend to reduce classifier accuracy relative to using empirically estimated priors (that is, allowing base rate differences to play a role in classification) because it increases the accuracy of rare terms at the expense of common ones. Nonetheless, we used uniform priors because they place all terms on a level footing and provide more interpretable results.

The estimate of P($A_j = 1$) reflects the regularization and the prior on term frequency:

$$p(A_j = 1) = p(A_j = 1 \mid T_k = 1)P(T_k = 1) + p(A_j = 1 \mid T_k = 0)P(T_k = 0)$$

where

$$p(A_j = 1 \mid T_k = 0) = \left( \sum_i A_{ij}(1 - T_{ik}) + m\mathrm{p} \right) \bigg/ \left( \sum_i (1 - T_{ik}) + m \right)$$

To ensure that only statistically robust associations were considered, all posterior probability maps were masked with the FDR-corrected *P*-value maps. For visualization purposes, thresholded maps were mapped to the PALS-B12 surface atlas[34] in SPM5 stereotaxic space. Average fiducial mapping values are presented. Datasets associated with **Figure 2** and **Supplementary Figure 3** are available in the SumsDB database (http://sumsdb.wustl.edu/sums/directory.do?id=8285126).

**Naive Bayes classifier.** We used a naive Bayes classifier[29] to predict the occurrence of specific terms using whole-brain patterns of activation. In classifier terminology, we have $n_S$ instances of feature-label pairs ($A_i$,$T_i$). The use of a naive Bayes classifier allows us to neglect the spatial dependence in the activation maps $A_i$. As simultaneous classification for the presence or absence of all $n_T$ terms is impractical owing to the larger number ($2^{n_T}$) of possible labels, for this work, we only considered mutually exclusive term labels, ranging from binary classification of two terms (for example, pain versus working memory) to multiclass classification of ten terms (for example, pain, working memory, language, conflict and so on).

For this setting we revised notation slightly from the previous section describing calculation of the posterior probability maps, letting scalar $T_i$ take values 1, …, $n_T{}^*$ for the subset of $n_T{}^*$ terms under consideration. For a new study with activation map A, the probability of term t is

$$P(T = t \mid A) = P(A \mid T = t)P(T = t) / P(A)$$

*P*(A) is computed as above for the studies under consideration, and by independence,

$$P(A \mid T = t) = \prod_j P(A_j \mid T = t),$$

and we use a regularized estimate for voxel *j*,

$$p(A_j = 1 \mid T = t) = \left( \sum_i A_{ij}I(T_i = t) + m\mathrm{p} \right) \bigg/ \left( \sum_i I(T_i = t) + m \right),$$

$$p(A_j = 0 \mid T = t) = 1 - P(A_j = 1 \mid T = t)$$

where *I*($\cdot$) is the indicator function (1 if the operand is true, 0 otherwise).

Although the assumption of conditional independence is usually violated in practice, leading to biased posterior probabilities, this generally does not affect classification performance because classification depends on the rank-ordered posterior probabilities of all classes rather than their absolute values. In complex real-world classification settings, naive Bayes classifiers often substantially outperform more sophisticated and computationally expensive techniques[35].

In the context of the present large-scale analyses, the naive Bayes classifier has several advantages over other widely used classification techniques (for example, support vector machines[36,37]). First, it requires substantially less training data than many other techniques because only the cross-classified cell counts are needed. Second, it is computationally efficient, and can scale up to extremely large sets of features (for example, hundreds of thousands of individual voxels) or possible outcomes without difficulty. Third, it produces easily interpretable results: the naive Bayes classifier's assumption of conditional independence ensures that the strength of each feature's contribution to the overall classification simply reflects the posterior probability of class membership conditioned on that feature (that is, P(T = t|$A_i$).

**Cross-validated classification of study-level maps.** For cross-validated classification of studies included in the NeuroSynth database (**Figs. 3** and **4**), we used the NBC to identify the most probable term from among a specified set of alternatives (for example, 'pain', 'emotion' and 'working memory') for each map. We used fourfold

cross-validation to ensure unbiased accuracy estimates. Because the database was known to contain errors, we took several steps to obtain more accurate classification estimates. First, to improve the signal-to-noise ratio, we trained and tested the classifier only on the subset of studies with at least 5,000 'active' voxels (that is, studies that satisfied $\Sigma_j A_{ij} \geq 5{,}000$) occurring when there were more than about four reported foci; $n_S = 2{,}107$ studies satisfied this criterion. This step ensured that studies with few reported activations (a potential marker of problems extracting coordinates) did not influence the classifier. Second, we only considered voxels that were activated in at least 3% of studies ($\Sigma_i A_{ij}/n_S \geq 0.03$), which ensured that noisy features would not exert undue influence on classification. Third, any studies in which more than one target term was used were excluded to ensure that there was always a correct answer (for example, if a study used both 'pain' and 'emotion' at a frequency of 0.001 or greater, it was excluded from classification). No further feature selection was used (all remaining voxels were included as features).

We calculated classifier accuracy by averaging across classes (terms) rather than studies (for example, if the classifier correctly classified 100% of 300 working memory studies, but 0% of 100 pain studies, we would report a value of 50%, reflecting the mean of 0% and 100%, rather than the study-wise mean of 75%, which allows for inflation due to differing numbers of studies). Using this accuracy metric, called balanced loss in the machine learning literature, eliminated the possibility of the classifier capitalizing on differences in term base rates and ensured that chance accuracy was always 50%. Note that this is the appropriate comparison for a naive Bayes classifier when uniform prior probabilities are stipulated because the classifier should not be able to capitalize on base rate differences even if they exist (as it has no knowledge of base rates beyond the specified prior).

For binary classification ($n_T^\star = 2$), we selected 25 terms that occurred at high frequency in our database (>1 in 1,000 words in at least 100 studies; **Fig. 5** and **Supplementary Fig. 3**) and ran the classifier on all possible pairs. For each pair, the set of studies used included all those with exactly one term present ($n_s = 23$–794; mean = 178.2, median = 141). Statistical significance for each pairwise classification was assessed using Monte Carlo simulation. Across all comparisons, the widest 95% confidence interval was 0.4–0.6, and the majority of observed classification accuracies (283/300) were statistically significant ($P < 0.05$; 257/300 were significant at $P < 0.001$).

For multiclass analyses involving $n_T^\star > 2$ terms (**Supplementary Fig. 5**), an exhaustive analysis of all possible combinations was not viable owing to combinatorial explosion and the increased processing time required. We therefore selected 100 random subsets of $n_T^\star$ terms from the larger set of 25, repeating the process for values of $n_T^\star$ between 3 and 10. All procedures were otherwise identical to those used for binary classification.

**Classification of single-subject data.** To classify single-subject data, we used data from several previous studies, including a large study of n-back working memory[38,39], five studies of emotional experience and reappraisal[40–44] and three studies of pain[14,45]. Methodological details for these studies can be found in the corresponding references. For working memory, we used single-subject contrasts that compared n-back working memory blocks to a fixation baseline. For emotion studies, we used single-subject contrast

maps that compared negative emotional pictures (from the IAPS set) to neutral pictures. For pain studies, we compared high and low thermal pain conditions.

Because the NBC was trained on binary maps (active vs. inactive) and single-subject $P$-maps varied continuously, all single-subject maps were binarized before classification. We used an arbitrary threshold of $P < 0.05$ to identify 'active' voxels. Because the maps on which the classifier was trained did not distinguish activations from deactivations, only positively activated voxels (n-back > fixation, negative emotion > neutral emotion or high pain > low pain) were considered active. Negatively activated voxels and nonsignificantly activated voxels were all considered inactive. To ensure that all single-subject maps had sufficient features for classification, we imposed a minimum cut-off of 1% of voxels—that is, for maps with fewer than 1% of voxels activated at $P < 0.05$, we used the top 1% of voxels, irrespective of threshold. Once the maps were binarized, all classification procedures were identical to those used for cross-validated classification of study-level maps.

The studies and contrasts included in the single-subject classification analysis were selected using objective criteria rather than on the (circular) basis of optimizing performance. The results we report include all studies that were subjected to the classifier (that is, we did not selectively include only studies that produced better results), despite the fact that there was marked heterogeneity within studies. For instance, one of the pain studies produced substantially better results ($n = 41$; sensitivity = 80%) than the other two (total $n = 34$; sensitivity = 47%), probably reflecting the fact that the former study contained many more trials per subject, resulting in more reliable single-subject estimates. Thus, the accuracy levels we report are arguably conservative, as they do not account for the potentially lower quality of some of our single-subject data.

Similarly, the contrasts we used for the three sets of studies were selected a priori on the basis of their perceived construct validity, and not on the basis of observed classification success. In fact, post-hoc analyses showed that alternative contrasts would have produced better results in some cases. Notably, for the emotion studies, using single-subject maps contrasting passive observation of negative IAPS pictures with active reappraisal of negative pictures would have improved classifier sensitivity somewhat (from 70% to 75%). Nonetheless, we opted to report the less favorable results in order to provide a reasonable estimate of single-subject classifier accuracy under realistic conditions, uncontaminated by selection bias. Future efforts to optimize the classifier for single-subject prediction (for example, by developing ways to avoid binarizing continuous maps, improving the quality of the automatically extracted data through manual verification and so on) would presumably lead to substantially better performance.

31. Van Essen, D.C. & Dierker, D.L. Surface-based and probabilistic atlases of primate cerebral cortex. *Neuron* **56**, 209–225 (2007).
32. Laird, A.R. *et al.* Comparison of the disparity between Talairach and MNI coordinates in functional neuroimaging data: validation of the Lancaster transform. *Neuroimage* **51**, 677–683 (2010).
33. Nigam, K., McCallum, A.K., Thrun, S. & Mitchell, T. Text classification from labeled and unlabeled documents using EM. *Mach. Learn.* **39**, 103–134 (2000).
34. Van Essen, D.C.A. Population-average, landmark- and surface-based (PALS) atlas of human cerebral cortex. *Neuroimage* **28**, 635–662 (2005).

35. Langley, P., Iba, W. & Thompson, K. An analysis of Bayesian classifiers. *Proceedings of the Tenth National Conference on Artificial Intelligence* 223–228 (AAAI Press, Menlo Park, California, USA, 1992).

36. Mitchell, T.M. *et al.* Learning to decode cognitive states from brain images. *Mach. Learn.* **57**, 145–175 (2004).

37. Cox, D.D. & Savoy, R.L. Functional magnetic resonance imaging (fMRI) "brain reading": detecting and classifying distributed patterns of fMRI activity in human visual cortex. *Neuroimage* **19**, 261–270 (2003).

38. DeYoung, C.G., Shamosh, N.A., Green, A.E., Braver, T.S. & Gray, J.R. Intellect as distinct from openness: differences revealed by fMRI of working memory. *J. Pers. Soc. Psychol.* **97**, 883–892 (2009).

39. Shamosh, N.A. *et al.* Individual differences in delay discounting. *Psychol. Sci.* **19**, 904–911 (2008).

40. McRae, K. *et al.* The neural bases of distraction and reappraisal. *J. Cogn. Neurosci.* **22**, 248–262 (2010).

41. Ochsner, K.N. *et al.* For better or for worse: neural systems supporting the cognitive down- and up-regulation of negative emotion. *Neuroimage* **23**, 483–499 (2004).

42. Ochsner, K.N., Bunge, S.A., Gross, J.J. & Gabrieli, J.D. Rethinking feelings: an FMRI study of the cognitive regulation of emotion. *J. Cogn. Neurosci.* **14**, 1215–1229 (2002).

43. Wager, T.D., Davidson, M.L., Hughes, B.L., Lindquist, M.A. & Ochsner, K.N. Prefrontal-subcortical pathways mediating successful emotion regulation. *Neuron* **59**, 1037–1050 (2008).

44. McRae, K., Ochsner, K.N., Mauss, I.B., Gabrieli, J.J.D. & Gross, J.J. Gender differences in emotion regulation: an fMRI study of cognitive reappraisal. *Group Process. Intergroup Relat.* **11**, 143–162 (2008).

45. Kross, E., Berman, M.G., Mischel, W., Smith, E.E. & Wager, T.D. Social rejection shares somatosensory representations with physical pain. *Proc. Natl. Acad. Sci. USA* **108**, 6270–6275 (2011).

doi:10.1038/nmeth.1635